

# **Analysis of Axisymmetric and Non-Axisymmetric Wave Propagation in a Homogeneous Piezoelectric Solid Circular Cylinder of Transversely Isotropic Material**

Michael Yu. Shatalov

*Sensor Science and Technology (SST) of the CSIR Material Science and Manufacturing,  
P.O. Box 395, Pretoria 0001, CSIR and*

*Department of Mathematics and Statistics of Tshwane University of Technology,  
P.B. X680, Pretoria 0001 FIN-40014, TUT  
South Africa*

## **1. Introduction**

Ultrasonic non-destructive evaluation relies on thorough understanding of the propagating and evanescent waves in the material under investigation. This study could be useful in such applications as, for example, the identification of defects of finite size across the circumference of a piezoelectric rod, since reflections of waves from such defects are generally non-axisymmetric in nature (Rose, 1999). Also, results obtained in this paper can serve as a basis for design of piezoelectric transducers, for which standing wave modes resulting from reflections of travelling waves at cross-section boundaries of the cylinder play an important role. The broad development of the finite (FEM) and boundary element methods (BEM) also needs some reference results obtained from exact solutions. In this case the proposed investigation of the non-axisymmetric propagating and evanescent waves in a piezoelectric cylinder could help to create reliable test beds of FEM and BEM.

The study of wave propagation in systems with cylindrical geometry has been undertaken by a number of investigators. While the systems considered so far have been both isotropic and anisotropic in nature, a relatively larger literature exists for isotropic materials. The first investigator of waves propagating in a solid isotropic cylinder was Pochhammer (Pochhammer, 1876). Other investigators of the subject can be found in standard texts (Achenbach, 1984), (Graff, 1991), and (Rose, 1999). For cylinders composed of anisotropic materials Chree (Chree, 1890) investigated propagation of the axisymmetric waves. Much later Mirsky (Mirsky, 1964) investigated a problem of non-axisymmetric wave propagation in transversely isotropic circular solid and hollow cylinders. Other contributors to the subject were (Armenakas & Reitz, 1973), (Frazer, 1980), (Nayfeh & Nagy (1995), (Berliner & Solecki, 1996), (Niklasson & Datta, 1998), and (Honarvar, et al., 2007), just to name a few. Numerical results for the dispersion of axisymmetric guided waves in a composite cylinder with a transversely isotropic core were presented by (Xu & Datta, 1991).

For piezoelectric cylinders the analysis of vibrations of circular shells was performed by Paul (Paul, 1966). Investigation of axisymmetric waves in layered piezoelectric rods with open circuit electric field conditions and their composites was carried out in (Nayfeh et al., 2000). The axisymmetric problem of the wave propagation in a piezoelectric transversely isotropic rod was analysed for rigid sliding and elastic simply supported mechanical boundary conditions and different types of electric field conditions in (Wei & Su, 2005). Several papers were devoted to development of numerical and finite element methods of investigation of piezoelectric cylinders. In (Siao et al., 1994) the authors solved the problem of wave propagation in a laminated piezoelectric cylinder via the FEM. Their paper contains tables and graphs of dispersion curves for real and imaginary values of wavenumbers. Unfortunately the data contains a misprint in a scale factor for the dimensionless wave number, making it quite difficult to compare their results with the results of the present paper. This misprint was further corrected in (Bai et al., 2004), who in their paper studied the electromechanical response of a laminated piezoelectric hollow cylinder by means of a semi-analytical FEM formulation. In (Shatalov & Loveday, 2004), and (Bai et al., 2006) the authors also studied the phenomenon of end reflections of waves in a semi-infinite layered piezoelectric cylinder.

Our approach parallels that of (Mirsky, 1964) and (Berliner & Solecki, 1996). It is also similar to (Winkel et al., 1995) who analytically solved the problem of wave propagations in an infinite cylindrical piezoelectric core rod immersed into an infinite piezoelectric cladding material. In (Winkel et al., 1995) the authors focused on the pure guided waves with real solutions of the determining bi-cubic equation. It was found in the process of investigation that this approach is applicable to the general problem of propagating and evanescent waves with real and complex solutions. In our approach the three dimensional equations of elastodynamics together with the quasi-electrostatic Gauss law are solved in terms of seven displacements and three electric potentials, each satisfying the Helmholtz equations. In contrast to (Winkel et al., 1995) we propose a simple approach to solution of the problem which has an additional advantage that in the limiting case of small electric and electromechanical constants our results automatically coincide with the classical results of (Mirsky, 1964) and (Berliner & Solecki, 1996) for a transversely isotropic cylinder. This evidence gives one confidence in the correctness of the obtained results. Imposing the allowed mechanical and electric boundary conditions on the cylinder surface, the characteristic or dispersion equation is derived in the form of a determinant of the fourth order in the non-axisymmetric case and a determinant of the third order in the axisymmetric case.

On the basis of the obtained results a numerical algorithm for displaying the dispersion curves is developed. The algorithm is based on calculation of the logarithm of modulus of the left hand side of the dispersion equation on a discrete mesh in the "wavenumber - frequency" ( $k - \omega$ ) plane. If the left hand side value of the dispersion equation tends to zero the logarithm tends to minus infinity. This method produces sharp negative spikes on the surface plot and automatically provides a picture of configuration of the dispersion curves. Similar approach of simultaneous qualitative displaying of the dispersion equation solutions was used in (Honarvar et al., 2006) that produced a 3-D cross-section of the real part of left hand side of the equation. The main advantage of our approach is that the local minima of the logarithm of modulus of the left hand side of the dispersion equation's matrix give proper approximations of the roots which can be further used as guess values of solutions of the dispersion equation. In the present chapter we present the dispersion curves of solid

cylinders made from two piezoelectric materials – PZT-4 and PZT-7A for open- and short-circuit electric boundary conditions and for different circumferential wavenumbers  $m = 1, 2, 3$  and for the axisymmetric case. The curves demonstrate substantial influence of the electric boundary conditions and electromechanical coupling on behaviour of the dispersion curves. These results obtained from exact solution of the problem could serve as the reference data and help researchers to create reliable FEM techniques for analysis of vibration of piezoelectric bodies.

## 2. Formulation of problem

In this section we establish the equations of motion and boundary conditions, and obtain solution of the problem within the framework of the following assumptions and approximations: linear elasticity, linear constitutional model of piezoelectricity, quasi-static approximation of the electric field, axial polarization of the piezoelectric material, neglecting of thermal effects, absence of free charges in the material, and boundary and body forces. Axis  $Oz$  coincides with the axis of the cylinder,  $r, \theta, z$  - radius, polar angle and axial coordinate, and  $u, v, w$  - radial, tangential and axial displacements correspondingly.

Equations of motion and boundary conditions of the cylindrical piezoelectric body are derived from the Hamilton variational principle. In order to apply Hamilton's principle we define the Lagrangian of the system as follows:

$$L = K - U + W \quad (1)$$

Where  $K$  is the kinetic energy,  $U$  is the strain energy and  $W$  is the electric energy of the system:

$$\begin{aligned} K &= \frac{\rho}{2} \int_{-\infty}^{\infty} \int_0^{2\pi} \int_0^a (u'^2 + v'^2 + w'^2) r dr d\theta dz, \\ U &= \frac{1}{2} \int_{-\infty}^{\infty} \int_0^{2\pi} \int_0^a (T_1 S_1 + T_2 S_2 + T_3 S_3 + T_4 S_4 + T_5 S_5 + T_6 S_6) r dr d\theta dz, \\ W &= \frac{1}{2} \int_{-\infty}^{\infty} \int_0^{2\pi} \int_0^a (D_1 E_1 + D_2 E_2 + D_3 E_3) r dr d\theta dz \end{aligned} \quad (2)$$

In these expressions  $u, v, w$  are the radial, tangential and axial displacements correspondingly,  $T_{1,2,\dots,6}$  are the stresses,  $S_{1,2,\dots,6}$  are the strains,  $D_{1,2,3}$  are the electric displacements and  $E_{1,2,3}$  are the electric fields. These components in the Voigt notation are:

$$\begin{aligned} T_1 &= c_{11}^E S_1 + c_{12}^E S_2 + c_{13}^E S_3 - e_{31} E_3, \\ T_2 &= c_{12}^E S_1 + c_{11}^E S_2 + c_{13}^E S_3 - e_{31} E_3, \\ T_3 &= c_{13}^E S_1 + c_{12}^E S_2 + c_{33}^E S_3 - e_{33} E_3, \\ T_4 &= c_{44}^E S_4 - e_{15} E_2, \quad T_5 = c_{44}^E S_5 - e_{15} E_1, \quad T_6 = c_{66}^E S_{66}, \end{aligned} \quad (3)$$

$$D_1 = \epsilon_{11}^S E_1 + e_{15} S_5, \quad D_2 = \epsilon_{11}^S E_2 + e_{15} S_4, \quad D_3 = \epsilon_{33}^S E_3 + e_{31} S_1 + e_{31} S_2 + e_{32} S_2$$

where  $c_{11}^E, c_{12}^E, c_{13}^E, c_{33}^E, c_{44}^E, c_{66}^E = (c_{11}^E - c_{12}^E)/2$  are the elastic stiffnesses at constant electric field,  $e_{15}, e_{31}$  are the piezoelectric constants or electromechanical coupling factors and  $\epsilon_{11}^S, \epsilon_{33}^S$  are the clamped dielectric constants at constant strain.

$$\begin{aligned} S_1 &= \frac{\partial u}{\partial r}, \quad S_2 = \frac{1}{r} \left( u + \frac{\partial v}{\partial \theta} \right), \quad S_3 = \frac{\partial w}{\partial z}, \quad S_4 = \frac{\partial v}{\partial z} + \frac{1}{r} \frac{\partial w}{\partial \theta}, \quad S_5 = \frac{\partial u}{\partial z} + \frac{\partial w}{\partial r}, \\ S_6 &= \frac{1}{r} \left( \frac{\partial u}{\partial \theta} - v \right) + \frac{\partial v}{\partial r}, \quad E_1 = -\frac{\partial \phi}{\partial r}, \quad E_2 = -\frac{1}{r} \frac{\partial \phi}{\partial \theta}, \quad E_3 = -\frac{\partial \phi}{\partial z} \end{aligned} \quad (4)$$

Substituting (2) – (3) into (1) the Lagrangian

$$L = \int_{-\infty}^{\infty} \int_0^{2\pi} \int_0^a \Lambda \, dr \, d\theta \, dz \quad (5)$$

is represented by the Lagrangian density  $\Lambda$ :

$$\Lambda = \Lambda(\dot{u}, \dot{v}, \dot{w}; u'_r, v'_r, w'_r, \phi'_r; u'_\theta, v'_\theta, w'_\theta, \phi'_\theta; u'_z, v'_z, w'_z, \phi'_z; u, v) \quad (6)$$

The Euler-Lagrange equations for Lagrangian (6) are:

$$\begin{aligned} \frac{\partial}{\partial t} \left( \frac{\partial \Lambda}{\partial \dot{u}} \right) + \frac{\partial}{\partial r} \left( \frac{\partial \Lambda}{\partial u'_r} \right) + \frac{\partial}{\partial \theta} \left( \frac{\partial \Lambda}{\partial u'_\theta} \right) + \frac{\partial}{\partial z} \left( \frac{\partial \Lambda}{\partial u'_z} \right) - \frac{\partial \Lambda}{\partial u} &= 0, \\ \frac{\partial}{\partial t} \left( \frac{\partial \Lambda}{\partial \dot{v}} \right) + \frac{\partial}{\partial r} \left( \frac{\partial \Lambda}{\partial v'_r} \right) + \frac{\partial}{\partial \theta} \left( \frac{\partial \Lambda}{\partial v'_\theta} \right) + \frac{\partial}{\partial z} \left( \frac{\partial \Lambda}{\partial v'_z} \right) - \frac{\partial \Lambda}{\partial v} &= 0, \\ \frac{\partial}{\partial t} \left( \frac{\partial \Lambda}{\partial \dot{w}} \right) + \frac{\partial}{\partial r} \left( \frac{\partial \Lambda}{\partial w'_r} \right) + \frac{\partial}{\partial \theta} \left( \frac{\partial \Lambda}{\partial w'_\theta} \right) + \frac{\partial}{\partial z} \left( \frac{\partial \Lambda}{\partial w'_z} \right) &= 0, \\ \frac{\partial}{\partial r} \left( \frac{\partial \Lambda}{\partial \phi'_r} \right) + \frac{\partial}{\partial \theta} \left( \frac{\partial \Lambda}{\partial \phi'_\theta} \right) + \frac{\partial}{\partial z} \left( \frac{\partial \Lambda}{\partial \phi'_z} \right) &= 0 \end{aligned} \quad (7)$$

Possible boundary conditions on the outer cylindrical surface obtained from the Hamilton principle are as follows:

$$\left. \frac{\partial \Lambda}{\partial u'_r} \right|_{r=a} = T_1|_{r=a} = 0 \quad (\text{cylindrical surface is free in the radial direction}) \text{ or} \quad (8a)$$

$$u|_{r=a} = 0 \quad (\text{cylindrical surface is clamped in the radial direction}) \quad (8b)$$

$$\left. \frac{\partial \Lambda}{\partial v'_r} \right|_{r=a} = T_6|_{r=a} = 0 \quad (\text{cylindrical surface is free in the tangential direction}) \text{ or} \quad (9a)$$

$$v|_{r=a} = 0 \quad (\text{cylindrical surface is clamped in the tangential direction}) \quad (9b)$$

$$\left. \frac{\partial \Lambda}{\partial w'_r} \right|_{r=a} = T_5|_{r=a} = 0 \quad (\text{cylindrical surface is free in the axial direction}) \text{ or} \quad (10a)$$

$$w|_{r=a} = 0 \quad (\text{cylindrical surface is clamped in the axial direction}) \quad (10b)$$

$$\left. \frac{\partial \Lambda}{\partial \phi'_r} \right|_{r=a} = D_1|_{r=a} = 0 \quad (\text{open-circuit conditions on the cylindrical surface}) \text{ or} \quad (11a)$$

$$\phi|_{r=a} = 0 \quad (\text{close-circuit electric boundary conditions on the cylindrical surface}) \quad (11b)$$

The Euler-Lagrange equation could be also presented in the standard form of the Navier equations of the linear dynamical elasticity (Redwood, 1960) and the Gauss law in the cylindrical coordinates:

$$\begin{aligned} \frac{\partial T_1}{\partial r} + \frac{1}{r} \frac{\partial T_6}{\partial \theta} + \frac{\partial T_5}{\partial z} + \frac{1}{r} (T_1 - T_2) &= \rho \ddot{u}, \\ \frac{\partial T_6}{\partial r} + \frac{1}{r} \frac{\partial T_2}{\partial \theta} + \frac{\partial T_4}{\partial z} + \frac{1}{r} T_6 &= \rho \ddot{v}, \\ \frac{\partial T_5}{\partial r} + \frac{1}{r} \frac{\partial T_4}{\partial \theta} + \frac{\partial T_3}{\partial z} + \frac{1}{r} T_5 &= \rho \ddot{w}, \\ \frac{\partial D_1}{\partial r} + \frac{1}{r} \left( D_1 + \frac{\partial D_2}{\partial \theta} \right) + \frac{\partial D_3}{\partial z} &= 0 \end{aligned} \quad (12)$$

Further we will assume that the outer cylindrical surface is free, hence, using (8a), (9a) and (10a) the boundary conditions are

$$T_1|_{r=a} = T_5|_{r=a} = T_6|_{r=a} = 0 \quad (13)$$

Electric boundary conditions will be considered in both open- and close-circuit form (11a) or (11b) and one of these conditions will be added to boundary conditions (13).

In the explicit form the system (9) or (12) of equations is as follows:

$$\begin{aligned} c_{11}^E \left( \frac{\partial^2 u}{\partial r^2} + \frac{1}{r} \frac{\partial u}{\partial r} - \frac{u}{r^2} - \frac{1}{r^2} \frac{\partial v}{\partial \theta} \right) + \frac{c_{12}^E}{r} \frac{\partial^2 v}{\partial r \partial \theta} + (c_{13}^E + c_{44}^E) \frac{\partial^2 w}{\partial r \partial z} + c_{44}^E \frac{\partial^2 u}{\partial z^2} \\ + c_{66}^E \left( \frac{1}{r^2} \frac{\partial^2 u}{\partial \theta^2} + \frac{1}{r} \frac{\partial^2 v}{\partial r \partial \theta} - \frac{1}{r^2} \frac{\partial v}{\partial \theta} \right) - e_{15} \frac{\partial E_1}{\partial z} - e_{31} \frac{\partial E_3}{\partial r} &= \rho \ddot{u}, \\ \frac{c_{11}^E}{r^2} \left( \frac{\partial u}{\partial \theta} + \frac{\partial^2 v}{\partial \theta^2} \right) + \frac{c_{12}^E}{r} \frac{\partial^2 u}{\partial r \partial \theta} + \frac{c_{13}^E + c_{44}^E}{r} \frac{\partial^2 w}{\partial \theta \partial z} + c_{44}^E \frac{\partial^2 v}{\partial z^2} \end{aligned}$$

$$\begin{aligned}
& + c_{66}^E \left( \frac{1}{r^2} \frac{\partial u}{\partial \theta} + \frac{1}{r} \frac{\partial^2 u}{\partial r \partial \theta} + \frac{\partial^2 v}{\partial r^2} + \frac{1}{r} \frac{\partial v}{\partial r} - \frac{v}{r^2} \right) - e_{15} \frac{\partial E_2}{\partial z} - \frac{e_{31}}{r} \frac{\partial E_3}{\partial \theta} = \rho \ddot{v}, \\
& (c_{13}^E + c_{44}^E) \left( \frac{1}{r} \frac{\partial u}{\partial z} + \frac{\partial^2 u}{\partial r \partial z} + \frac{1}{r} \frac{\partial^2 v}{\partial r \partial \theta} \right) + c_{44}^E \left( \frac{\partial^2 w}{\partial r^2} + \frac{1}{r} \frac{\partial w}{\partial r} + \frac{1}{r^2} \frac{\partial^2 w}{\partial \theta^2} \right) + c_{33}^E \frac{\partial^2 w}{\partial z^2} \\
& - e_{15} \left( \frac{\partial E_1}{\partial r} + \frac{E_1}{r} - \frac{1}{r} \frac{\partial E_3}{\partial \theta} \right) - e_{33} \frac{\partial E_3}{\partial z} = \rho \ddot{w}, \\
e_{15} & \left( \frac{\partial^2 u}{\partial r \partial z} + \frac{1}{r} \frac{\partial u}{\partial r} + \frac{1}{r} \frac{\partial^2 v}{\partial \theta \partial z} + \frac{\partial^2 w}{\partial r^2} + \frac{1}{r} \frac{\partial w}{\partial r} + \frac{1}{r^2} \frac{\partial^2 w}{\partial \theta \partial z} \right) + e_{31} \left( \frac{1}{r} \frac{\partial u}{\partial z} + \frac{\partial^2 v}{\partial r \partial z} + \frac{1}{r} \frac{\partial^2 w}{\partial \theta \partial z} \right) \\
& + \varepsilon_{11}^S \left( \frac{\partial E_1}{\partial r} + \frac{E_1}{r} + \frac{1}{r} \frac{\partial E_2}{\partial \theta} \right) + \varepsilon_{33}^S \frac{\partial E_3}{\partial z} = 0
\end{aligned} \tag{14}$$

The explicit form of boundary conditions (13) is:

$$\begin{aligned}
T_1|_{r=a} &= \left[ c_{11}^E \frac{\partial u}{\partial r} + c_{12}^E \left( \frac{1}{r} \left( u + \frac{\partial v}{\partial \theta} \right) \right) + c_{13}^E \left( \frac{\partial w}{\partial z} \right) + e_{31} \left( \frac{\partial \phi}{\partial z} \right) \right]_{r=a} = 0, \\
T_5|_{r=a} &= \left[ c_{44}^E \left( \frac{\partial u}{\partial z} + \frac{\partial w}{\partial r} \right) + e_{15} \frac{\partial \phi}{\partial r} \right]_{r=a} = 0, \quad T_6|_{r=a} = c_{66}^E \left[ \frac{1}{r} \left( \frac{\partial u}{\partial \theta} - v \right) + \frac{\partial v}{\partial r} \right]_{r=a} = 0 \tag{15} \\
D_1|_{r=a} &= \left[ -\varepsilon_{11}^S \frac{\partial \phi}{\partial r} + e_{15} \left( \frac{\partial u}{\partial z} + \frac{\partial w}{\partial r} \right) \right]_{r=a} = 0 \quad \text{or} \quad \phi|_{r=a} = 0
\end{aligned}$$

### 3. Analytic solution of the problem

We seek the solution of the problem (14) – (15) in terms of harmonic travelling waves along  $Z$ -axis in terms of several displacement and electric potentials first introduced by (Mirsky, 1964) and further used by (Winkel et al 1995) and (Shatalov et al., 2009) as follows:

$$\begin{aligned}
u &= u(r, \theta, z, t) = \left[ \frac{\partial \varphi(r, \theta)}{\partial r} + \frac{1}{r} \frac{\partial \psi(r, \theta)}{\partial \theta} \right] e^{i(\omega t + kr)}, \\
v &= v(r, \theta, z, t) = \left[ \frac{1}{r} \frac{\partial \varphi(r, \theta)}{\partial \theta} - \frac{\partial \psi(r, \theta)}{\partial r} \right] e^{i(\omega t + kr)}, \\
w &= w(r, \theta, z, t) = \chi(r, \theta) e^{i(\omega t + kr)}, \quad \phi = \phi(r, \theta, z, t) = \tau(r, \theta) e^{i(\omega t + kr)}
\end{aligned} \tag{16}$$

where  $\varphi(r, \theta)$ ,  $\psi(r, \theta)$ ,  $\chi(r, \theta)$  and  $\tau(r, \theta)$  are unknown potentials.

After substitution (16) into (14) we obtain the following system of equations:

$$\frac{\partial}{\partial r} \left\{ \left[ c_{11}^E \nabla^2 \varphi + (\rho \omega^2 - k^2 c_{44}^E) \varphi \right] + \left[ ik (c_{13}^E + c_{44}^E) \chi \right] + \left[ ik (e_{15} + e_{31}) \tau \right] \right\}$$

$$\begin{aligned}
 & + \frac{1}{r} \frac{\partial}{\partial \theta} \left\{ \left[ c_{66}^E \nabla^2 \psi + (\rho \omega^2 - k^2 c_{44}^E) \psi \right] \right\} = 0, \\
 & \frac{1}{r} \frac{\partial}{\partial \theta} \left\{ \left[ c_{11}^E \nabla^2 \varphi + (\rho \omega^2 - k^2 c_{44}^E) \varphi \right] + \left[ ik(c_{13}^E + c_{44}^E) \chi \right] + \left[ ik(e_{15} + e_{31}) \tau \right] \right\} \\
 & - \frac{\partial}{\partial r} \left\{ \left[ c_{66}^E \nabla^2 \psi + (\rho \omega^2 - k^2 c_{44}^E) \psi \right] \right\} = 0, \\
 & \left[ ik(c_{13}^E + c_{44}^E) \nabla^2 \varphi \right] + \left[ c_{44}^E \nabla^2 \chi + (\rho \omega^2 - k^2 c_{33}^E) \chi \right] + \left[ e_{15} \nabla^2 \tau - k^2 e_{33} \tau \right] = 0, \\
 & \left[ ik(e_{15} + e_{31}) \nabla^2 \varphi \right] + \left[ e_{15} \nabla^2 \chi - k^2 e_{33} \chi \right] - \left[ \varepsilon_{11} \nabla^2 \tau - k^2 \varepsilon_{33} \tau \right] = 0
 \end{aligned} \tag{17}$$

where  $\nabla^2 = \frac{\partial^2}{\partial r^2} + \frac{1}{r} \frac{\partial}{\partial r} + \frac{1}{r^2} \frac{\partial^2}{\partial \theta^2}$  is the two dimensional Laplace operator in polar coordinates.

The first two equations of systems (17) are satisfied if

$$c_{66}^E \nabla^2 \psi + (\rho \omega^2 - k^2 c_{44}^E) \psi = 0, \tag{18}$$

$$\left[ c_{11}^E \nabla^2 \varphi + (\rho \omega^2 - k^2 c_{44}^E) \varphi \right] + \left[ ik(c_{13}^E + c_{44}^E) \chi \right] + \left[ ik(e_{15} + e_{31}) \tau \right] = 0$$

First equation of system (18) is separated from the second equation as well as from the third and fourth equations of system (17). It could be represented as the Helmholtz equation in the polar coordinates:

$$\nabla^2 \psi + \zeta_0^2 \psi = 0 \tag{19}$$

$$\text{where } \zeta_0^2 = \frac{\rho \omega^2 - k^2 c_{44}^E}{c_{66}^E}.$$

Second equation of system (18) must be compatible with the third and fourth equations of system (17), i.e. we have the following system of equations:

$$\begin{aligned}
 & \left[ c_{11}^E \nabla^2 \varphi + (\rho \omega^2 - k^2 c_{44}^E) \varphi \right] + \left[ ik(c_{13}^E + c_{44}^E) \chi \right] + \left[ ik(e_{15} + e_{31}) \tau \right] = 0, \\
 & \left[ ik(c_{13}^E + c_{44}^E) \nabla^2 \varphi \right] + \left[ c_{44}^E \nabla^2 \chi + (\rho \omega^2 - k^2 c_{33}^E) \chi \right] + \left[ e_{15} \nabla^2 \tau - k^2 e_{33} \tau \right] = 0, \\
 & \left[ ik(e_{15} + e_{31}) \nabla^2 \varphi \right] + \left[ e_{15} \nabla^2 \chi - k^2 e_{33} \chi \right] - \left[ \varepsilon_{11} \nabla^2 \tau - k^2 \varepsilon_{33} \tau \right] = 0
 \end{aligned} \tag{20}$$

To solve this system of equations we try to represent them in the form of the Helmholtz equation as (19):

$$\nabla^2 \varphi + \zeta^2 \varphi = 0, \quad \nabla^2 \chi + \zeta^2 \chi = 0, \quad \nabla^2 \tau + \zeta^2 \tau = 0 \tag{21}$$

where  $\zeta^2$  is unknown parameter which will be calculated after substitution (21) in (20). Substituting  $\nabla^2 \varphi = -\zeta^2 \varphi$ ,  $\nabla^2 \chi = -\zeta^2 \chi$  and  $\nabla^2 \tau = -\zeta^2 \tau$  into (20) we obtain the following system of equation for determination of parameter  $\zeta^2$ :

$$\begin{aligned} & \left[ (\rho\omega^2 - k^2 c_{44}^E) - c_{11}^E \zeta^2 \right] \varphi + \left[ i k (c_{13}^E + c_{44}^E) \right] \chi + \left[ i k (e_{15} + e_{31}) \right] \tau = 0, \\ & \left[ -i k (c_{13}^E + c_{44}^E) \zeta^2 \right] \varphi + \left[ (\rho\omega^2 - k^2 c_{33}^E) - c_{44}^E \zeta^2 \right] \chi + \left[ -(k^2 e_{33}) - e_{15} \zeta^2 \right] \tau = 0, \\ & \left[ -i k (e_{15} + e_{31}) \zeta^2 \right] \varphi + \left[ -(k^2 e_{33}) - \zeta^2 \right] \chi + \left[ (k^2 \varepsilon_{33}) + \zeta^2 \varepsilon_{11} \right] \tau = 0 \end{aligned} \quad (22)$$

System (22) has nontrivial solutions if the determinant of the system is zero:

$$\begin{vmatrix} (\rho\omega^2 - k^2 c_{44}^E) - c_{11}^E \zeta^2 & i k (c_{13}^E + c_{44}^E) & i k (e_{15} + e_{31}) \\ -i k (c_{13}^E + c_{44}^E) \zeta^2 & (\rho\omega^2 - k^2 c_{33}^E) - c_{44}^E \zeta^2 & -(k^2 e_{33}) - e_{15} \zeta^2 \\ -i k (e_{15} + e_{31}) \zeta^2 & -(k^2 e_{33}) - \zeta^2 & (k^2 \varepsilon_{33}) + \zeta^2 \varepsilon_{11} \end{vmatrix} = 0 \quad (23)$$

Hence the unknown values of  $\zeta^2$  are calculated from this determining equation which could be rewritten in the form of the bi-cubic determining equation:

$$(\zeta^2)^3 + b_1 (\zeta^2)^2 + b_2 (\zeta^2) + b_3 = 0 \quad (24)$$

where

$$\begin{aligned} b_1 &= \frac{-\rho\omega^2 B_1 + k^2 B_2}{B_0}, & b_2 &= \frac{\varepsilon_{11} (\rho\omega^2)^2 - k^2 (\rho\omega^2) B_3 + k^4 B_4}{B_0}, \\ b_3 &= \frac{k^2 (k^2 c_{44}^E - \rho\omega^2) \left[ k^2 B_5 - (\rho\omega^2) \varepsilon_{33} \right]}{B_0}, & B_0 &= c_{11}^E (e_{15}^2 + \varepsilon_{11} c_{44}^E), \\ B_1 &= e_{15}^2 + \varepsilon_{11} (c_{11}^E + c_{44}^E), & B_3 &= \varepsilon_{11} (c_{33}^E + c_{44}^E) + \varepsilon_{33} (c_{11}^E + c_{44}^E) + (e_{15} + e_{31})^2 + 2e_{15} e_{33}, \\ B_2 &= \varepsilon_{11} \left( c_{11}^E c_{33}^E - 2c_{13}^E c_{44}^E - (c_{13}^E)^2 \right) + 2e_{15} (c_{11}^E e_{33} - c_{13}^E e_{31}) + c_{44}^E (e_{31}^2 + \varepsilon_{33} c_{11}^E) - 2c_{13}^E e_{15}^2, \\ B_4 &= -(c_{13}^E)^2 \varepsilon_{33} - 2c_{13}^E \left[ e_{33} (e_{15} + e_{31}) - c_{44}^E \varepsilon_{33} \right] + c_{33}^E \left[ (e_{15} + e_{33})^2 + c_{44}^E \varepsilon_{11} + c_{11}^E \varepsilon_{33} \right] + c_{11}^E \varepsilon_{33}^2 - 2c_{44}^E e_{31} e_{33}, \\ B_5 &= c_{33}^E \varepsilon_{11} + e_{33}^2 \end{aligned} \quad (25)$$

Hence, in general case we have three different solutions of bi-cubic equation (24)  $\zeta_1^2$ ,  $\zeta_2^2$  and  $\zeta_3^2$ :

$$\zeta_1^2 = -\frac{b_1}{3} + (A + B), \quad \zeta_{2,3}^2 = -\frac{b_1}{3} - \frac{A + B}{2} \pm i \frac{A - B}{2} \sqrt{3} \quad (26)$$

where

$$A = \sqrt[3]{-\frac{q}{2} + \sqrt{Q}}, \quad B = \sqrt[3]{-\frac{q}{2} - \sqrt{Q}}, \quad (27)$$

$$Q = \frac{p^3}{27} + \frac{q^2}{4}, \quad p = -\frac{b_1^3}{3} + b_2, \quad q = \frac{2b_1^3}{27} - \frac{b_1 b_2}{3} + b_3$$

Hence, we have three independent Helmholtz equations:

$$\nabla^2 \phi_j + \zeta_j^2 \phi_j = 0, \quad (j = 1, 2, 3) \quad (28)$$

It follows from equations (20) - (22) that functionals  $\chi_j = \chi_j(r, \theta)$  and  $\tau_j = \tau_j(r, \theta)$  in expressions (17) - (18) and (20) - (22) could be calculated as follows:

$$\chi_j = \chi_j(r, \theta) = \eta_j \varphi_j(r, \theta), \quad \tau_j = \tau_j(r, \theta) = \mu_j \varphi_j(r, \theta) \quad (29)$$

where coefficients  $\eta_j$ ,  $\mu_j$  are obtained from system of equations (22) after substitution expressions (29):

$$\begin{aligned} & \left[ ik(c_{13}^E + c_{44}^E) \right] \eta_j + \left[ ik(e_{15} + e_{31}) \right] \mu_j = - \left[ (\rho\omega^2 - k^2 c_{44}^E) - c_{11}^E \zeta_j^2 \right], \\ & \left[ (\rho\omega^2 - k^2 c_{33}^E) - c_{44}^E \zeta_j^2 \right] \eta_j + \left[ -(k^2 e_{33}) - e_{15} \zeta_j^2 \right] \mu_j = \left[ ik(c_{13}^E + c_{44}^E) \zeta_j^2 \right], \\ & \left[ -(k^2 e_{33}) - \zeta_j^2 \right] \eta_j + \left[ (k^2 \varepsilon_{33}) + \zeta_j^2 \varepsilon_{11} \right] \mu_j = \left[ ik(e_{15} + e_{31}) \zeta_j^2 \right] \end{aligned} \quad (30)$$

For example, we can find  $\eta_j$  from the first and second equations of (30) and  $\mu_j$  from the third equation of this system:

$$\begin{aligned} \eta_j &= \eta_j(k, \omega) = -\frac{i}{k} \frac{\zeta_j^4 c_{11}^E e_{15} + \zeta_j^2 \left[ k^2 B_6 - (\rho\omega^2) e_{15} \right] + k^2 (k^2 c_{44}^E - \rho\omega^2) e_{33}}{k^2 B_7 + \zeta_j^2 B_8 + \rho\omega^2 B_9}, \\ \mu_j &= \mu_j(k, \omega) = \frac{\zeta_j^2 \left[ \eta_j e_{15} - i k B_9 \right] + k^2 \eta_j e_{33}}{\zeta_j^2 \varepsilon_{11} + k^2 \varepsilon_{33}}, \quad (j = 1, 2, 3) \end{aligned} \quad (31)$$

where

$$\begin{aligned} B_6 &= c_{11}^E e_{33} - c_{13}^E e_{15} + (c_{13}^E + c_{44}^E) e_{31}, & B_7 &= (c_{13}^E + c_{44}^E) e_{33} - c_{13}^E (e_{15} + e_{31}), \\ B_8 &= c_{13}^E e_{15} - c_{44}^E e_{31}, & B_9 &= e_{15} + e_{31} \end{aligned} \quad (32)$$

Finally the solution of system (14) using representation (16) is as follows:

$$\begin{aligned} u &= u(r, \theta, z, t) = \left[ \frac{1}{r} \frac{\partial \psi(r, \theta)}{\partial \theta} + \frac{\partial \varphi_1(r, \theta)}{\partial r} + \frac{\partial \varphi_2(r, \theta)}{\partial r} + \frac{\partial \varphi_3(r, \theta)}{\partial r} \right] e^{i(\omega t + kr)}, \\ v &= v(r, \theta, z, t) = \left[ -\frac{\partial \psi(r, \theta)}{\partial r} + \frac{1}{r} \frac{\partial \varphi_1(r, \theta)}{\partial \theta} + \frac{1}{r} \frac{\partial \varphi_2(r, \theta)}{\partial \theta} + \frac{1}{r} \frac{\partial \varphi_3(r, \theta)}{\partial \theta} \right] e^{i(\omega t + kr)}, \\ w &= w(r, \theta, z, t) = [\eta_1 \varphi_1(r, \theta) + \eta_2 \varphi_2(r, \theta) + \eta_3 \varphi_3(r, \theta)] e^{i(\omega t + kr)}, \end{aligned} \quad (33)$$

$$\phi = \phi(r, \theta, z, t) = [\mu_1 \varphi_1(r, \theta) + \mu_2 \varphi_2(r, \theta) + \mu_3 \varphi_3(r, \theta)] e^{i(\omega t + kr)}$$

Solution of the Helmholtz equations (19):  $\nabla^2 \psi + \zeta_0^2 \psi = 0$  and (28):  $\nabla^2 \varphi_j + \zeta_j^2 \varphi_j = 0$ , ( $j = 1, 2, 3$ ) for the solid cylinder is:

$$\psi = \psi(r, \theta) = A_0 W_m(\zeta_0 r) \sin(m\theta + \theta_0), \quad \varphi_j = \varphi_j(r, \theta) = A_j W_m(\zeta_j r) \cos(m\theta + \theta_0) \quad (34)$$

where  $m$  is a positive integer in the non-axisymmetric case,  $A_j$  - arbitrary constants, representing the circumferential wave number,  $W_m(\zeta r) = J_m(\zeta r)$  is the Bessel function of the first kind if  $\zeta$  is real or complex and  $W_m(\zeta r) = I_m(|\zeta|r)$  is the Bessel function of the second kind if  $\zeta$  is pure imaginary number.

Mechanical boundary conditions correspond to the assumption of absence of external forces on the cylindrical boundary:

$$T_1|_{r=a} = T_5|_{r=a} = T_6|_{r=a} = 0 \quad (35)$$

There are two types of electric boundary conditions:

$$D_1|_{r=a} = 0 \quad \text{or} \quad \phi|_{r=a} = 0 \quad (36)$$

where the first expression corresponds to the open-circuit condition and the second expression - to the close-circuit condition.

After substitution (34) into (33), (4), and (3) we obtain two systems of four linear homogeneous algebraic equations in the unknown amplitudes  $A_{0,1,2,3}$ . Each of these systems of equations has a non-trivial solution if and only if its main determinant equals zero:

$$Det(k, \omega) = \begin{vmatrix} a_{11} & a_{12} & a_{13} & a_{14} \\ a_{21} & a_{22} & a_{23} & a_{24} \\ a_{31} & a_{32} & a_{33} & a_{34} \\ a_{41} & a_{42} & a_{43} & a_{44} \end{vmatrix} = 0 \quad (37)$$

where  $a_{j1,j2} = a_{j1,j2}(k, \omega)$  ( $j1, j2 = 1, 2, 3, 4$ ) are given in the Appendix. Equation (37) forms the dispersion equation.

*Remark on limiting case of small electro-mechanical coupling coefficients.* If electro-mechanical coupling coefficients  $e_{15} = e_{31} = e_{33} = 0$  the determining equation (24) is converted into

$$\left[ (\xi_j^2) - k^2 \frac{\varepsilon_{33}}{\varepsilon_{11}} \right] \left[ (\xi_j^2)^2 + b_4 (\xi_j^2) + b_5 \right] = 0 \quad (38)$$

where

$$b_4 = \frac{-(\rho \omega^2) B_{11} + k^2 B_{12}}{B_{10}}, \quad b_5 = \frac{[(\rho \omega^2) - k^2 c_{33}^E][( \rho \omega^2) - k^2 c_4^E]}{B_{10}},$$

$$B_{10} = c_{11}^E c_{44}^E, \quad B_{11} = c_{11}^E + c_{44}^E, \quad B_{12} = c_{11}^E c_{33}^E - (c_{13}^E)^2 - 2c_{13}^E c_{44}^E \quad (39)$$

Hence in (17) the electric and mechanical parts are separated and the determining equation  $(\xi_j^2)^2 + b_4(\xi_j^2) + b_5 = 0$  describes the wave dynamics in the passive transversely isotropic medium. This equation coincides with the corresponding equation (Berliner & Solecki, 1996) and hence, all the presented results are converted into the well known results (Mirsky, 1964) and (Berliner & Solecki, 1996) in the limiting case of small electro-mechanical coupling coefficients. Additional dispersion line, corresponding to  $(\xi_j^2)\varepsilon_{11} - k^2\varepsilon_{33} = 0$  could be considered as an artefacts in this case.

Furthermore if we suppose that  $e_{15} = e_{31} = 0$  in the first expression (31) we obtain that

$$\eta_j = \frac{i(\rho\omega^2) - (\zeta_j^2)c_{11}^E - k^2c_{44}^E}{k(c_{13}^E + c_{44}^E)} \quad (40)$$

which also coincides with the known result (Berliner & Solecki, 1996). Hence, the results obtained contain the classical results of investigation of a passive transversely isotropic material as a particular limiting case.

#### 4. Axisymmetric case

Axisymmetric vibrations of the piezoelectric cylinder could be considered as a particular case of the general problem with  $m = 0$ ,  $v = 0$ ,  $E_2 = 0$ ,  $T_4 = T_6 = 0$  and all variables are  $\theta$ -independent.

In this case system of equations (14) is rewritten as follows:

$$\begin{aligned} c_{11}^E \left( \frac{\partial^2 u}{\partial r^2} + \frac{1}{r} \frac{\partial u}{\partial r} - \frac{u}{r^2} \right) + (c_{13}^E + c_{44}^E) \frac{\partial^2 w}{\partial r \partial z} + c_{44}^E \frac{\partial^2 u}{\partial z^2} - e_{15} \frac{\partial E_1}{\partial z} - e_{31} \frac{\partial E_3}{\partial r} &= \rho \ddot{u}, \\ (c_{13}^E + c_{44}^E) \left( \frac{1}{r} \frac{\partial u}{\partial z} + \frac{\partial^2 u}{\partial r \partial z} \right) + c_{44}^E \left( \frac{\partial^2 w}{\partial r^2} + \frac{1}{r} \frac{\partial w}{\partial r} \right) + c_{33}^E \frac{\partial^2 w}{\partial z^2} - e_{15} \left( \frac{\partial E_1}{\partial r} + \frac{E_1}{r} \right) - e_{33} \frac{\partial E_3}{\partial z} &= \rho \ddot{w}, \\ e_{15} \left( \frac{\partial^2 u}{\partial r \partial z} + \frac{1}{r} \frac{\partial u}{\partial r} + \frac{\partial^2 w}{\partial r^2} + \frac{1}{r} \frac{\partial w}{\partial r} \right) + e_{31} \left( \frac{1}{r} \frac{\partial u}{\partial z} + \frac{\partial^2 v}{\partial r \partial z} \right) + \varepsilon_{11}^S \left( \frac{\partial E_1}{\partial r} + \frac{E_1}{r} \right) + \varepsilon_{33}^S \frac{\partial E_3}{\partial z} &= 0 \end{aligned} \quad (41)$$

Boundary conditions (15) are:

$$\begin{aligned} T_1|_{r=a} &= \left[ c_{11}^E \left( \frac{\partial u}{\partial r} \right) + c_{12}^E \left( \frac{u}{r} \right) + c_{13}^E \left( \frac{\partial w}{\partial z} \right) + e_{31} \left( \frac{\partial \phi}{\partial z} \right) \right]_{r=a} = 0, \\ T_5|_{r=a} &= \left[ c_{44}^E \left( \frac{\partial u}{\partial z} + \frac{\partial w}{\partial r} \right) + e_{15} \frac{\partial \phi}{\partial r} \right]_{r=a} = 0, \\ D_1|_{r=a} &= \left[ -\varepsilon_{11}^S \frac{\partial \phi}{\partial r} + e_{15} \left( \frac{\partial u}{\partial z} + \frac{\partial w}{\partial r} \right) \right]_{r=a} = 0 \quad \text{or} \quad \phi|_{r=a} = 0 \end{aligned} \quad (42)$$

The variables are changed as follows:

$$u = u(r, z, t) = \left[ \frac{\partial \varphi(r)}{\partial r} \right] e^{i(\omega t + kr)}, \quad w = w(r, z, t) = \chi(r) e^{i(\omega t + kr)},$$

$$\phi = \phi(r, z, t) = \tau(r) e^{i(\omega t + kr)} \quad (43)$$

and system of equations (20) is obtained. All relationships (21) – (32) are true for the axisymmetric case and the final representation of solutions of system (41) is:

$$u = u(r, z, t) = \left[ \frac{\partial \varphi_1(r)}{\partial r} + \frac{\partial \varphi_2(r)}{\partial r} + \frac{\partial \varphi_3(r)}{\partial r} \right] e^{i(\omega t + kr)},$$

$$w = w(r, z, t) = [\eta_1 \varphi_1(r) + \eta_2 \varphi_2(r) + \eta_3 \varphi_3(r)] e^{i(\omega t + kr)}, \quad (44)$$

$$\phi = \phi(r, z, t) = [\mu_1 \varphi_1(r) + \mu_2 \varphi_2(r) + \mu_3 \varphi_3(r)] e^{i(\omega t + kr)}$$

Solution of the Helmholtz equations (28):  $\nabla^2 \varphi_j + \zeta_j^2 \varphi_j = 0$ , ( $j = 1, 2, 3$ ) is:

$$\varphi_j = \varphi_j(r) = A_j W_m(\zeta_j r) \quad (45)$$

where  $A_j$  - arbitrary constants, representing the circumferential wave number,  $W_m(\zeta_j r) = J_m(\zeta_j r)$  is the Bessel function of the first kind if  $\zeta_j$  is real or complex and  $W_m(\zeta_j r) = I_m(|\zeta_j| r)$  is the Bessel function of the second kind if  $\zeta_j$  is pure imaginary number.

Boundary conditions are obtained from determinant (37) by means of elimination of third row and fourth column.

## 5. Numerical results and discussion

In this section we present the dispersion curves for non-axisymmetric waves with circumferential wavenumbers  $m = 1, 2, 3$  and axisymmetric waves resulting from the characteristic equation (38). Two piezoelectric materials are chosen, PZT-4 and PZT-7A, to illustrate the influence of electro-mechanical coupling coefficients on the configuration of the dispersion curves. The relevant material parameters for PZT-4 and PZT-7A are given in the Table 1.

In order to obtain the dispersion curves we made use of a method similar to the novel method (Honarvar et al., 2008) where the dispersion curves are not produced as a result of solving of the dispersion equation by a traditional iterative find-root algorithm but are obtained by a zero-level cut in the velocity-frequency plane. In this chapter we modify this approach calculating the logarithm of modulus of determinant (37) on the mesh  $(k_{j1}, \omega_{j2})$ ,  $j1 = 1, \dots, N_1; j2 = 1, \dots, N_2$  (Shatalov et al., 2009). In those points where the real and imaginary parts of determinant (37) are close to zero substantial negative spikes occur which are displayed on a surface plot and give a picture of the configuration of the dispersion curves. The main advantage of this approach is that the local minima of the  $[N_1 \times N_2]$  - matrix of the logarithms are the proper guess values of the dispersion equation's

Geometric and Material Constants	PZT-4	PZT-7A	SI Units
Radius ( $a$ )	1	1	$m$
( $\rho$ )	$7.5 \cdot 10^3$	$7.6 \cdot 10^3$	$kg/m^3$
$c_{11}^E$	$13.9 \cdot 10^{10}$	$14.8 \cdot 10^{10}$	$N/m^2$
$c_{12}^E$	$7.78 \cdot 10^{10}$	$7.62 \cdot 10^{10}$	$N/m^2$
$c_{13}^E$	$7.43 \cdot 10^{10}$	$7.42 \cdot 10^{10}$	$N/m^2$
$c_{33}^E$	$11.5 \cdot 10^{10}$	$13.1 \cdot 10^{10}$	$N/m^2$
$c_{44}^E$	$2.56 \cdot 10^{10}$	$2.53 \cdot 10^{10}$	$N/m^2$
$e_{15}$	12.7	9.2	$C/m^2$
$e_{31}$	-5.2	-2.1	$C/m^2$
$e_{33}$	15.1	9.5	$C/m^2$
$\varepsilon_{11}^S$	$730 \cdot \varepsilon_0$	$460 \cdot \varepsilon_0$	$C^2 m^{-2} N^{-1}$
$\varepsilon_{33}^S$	$635 \cdot \varepsilon_0$	$235 \cdot \varepsilon_0$	$C^2 m^{-2} N^{-1}$

Table. Material constants and geometric parameters for PZT-4 and PZT-7A  
 $(\varepsilon_0 = 8.85 \cdot 10^{-12} C^2 m^{-2} N^{-1})$

roots. Hence all roots of equation (37) could be found for values of wavenumbers ( $k_{j_1}$ ) on the real axis and on or near the imaginary axis as a function of frequency ( $\omega_{j_2}$ ). Another advantage of this method is that it is much faster than the traditional root finding methods and as fast as the Honarvar method (Honarvar et al., 2008).

The main disadvantage of this approach is that the roots of characteristic arguments ( $\xi_j$ ), ( $j = 0, 1, 2, 3$ ) are also displayed on the surface plots as obvious artefacts. An elaborate discussion of these artefacts is given by Yenwong-Fai, (Yenwong-Fai, 2008). These artefacts could be simply detected and eliminated from the dispersion plots by program tools. Our algorithm, as it has been implemented, does not search for branches of the dispersion relation well away from the real and imaginary axes for  $k$ . It would be relatively straightforward in principle to locate these additional branches.

Dispersion curves of bending waves ( $m=1$ ) in the cylinder made from PZT-4 with the short-circuit lateral (cylindrical) surface are depicted in Fig. 1 in dimensionless coordinates  $(k \cdot a \div \Omega = \omega / (a \cdot V_s))$ , where  $V_s = \sqrt{c_{44}^E / \rho}$ , and  $a$  is the outer radius of the cylinder. The picture of the dispersion curves is obtained by a method described above for real (propagating waves) and pure imaginary values of the wavenumber in the limits:  $\text{Re}(k \cdot a), \text{Im}(k \cdot a) \in (0, 8]$ ,  $\Omega = \omega / (a \cdot V_s) \in (0, 14]$  with resolution 500 (250 pixels for real and 250 pixels for imaginary ( $k \cdot a$ ))  $\times$  250 ( $\Omega = \omega / (a \cdot V_s)$ ) pixels. The same resolution is used for Fig. 2 - 17.

The first dispersion curve of the propagating waves (real values of the wavenumber) tends to an asymptote of the surface wave propagation. It is joined to the second curve which tends to the asymptote of the shear waves through the domain of the evanescent waves.

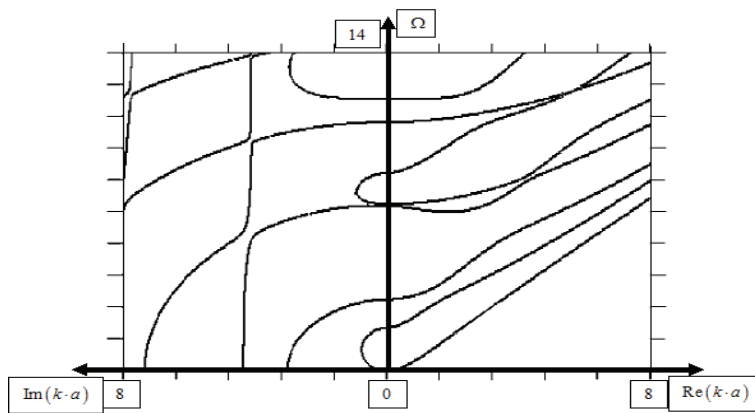


Fig. 1. PZT-4 cylinder with short-circuit lateral surface ( $m = 1$ )

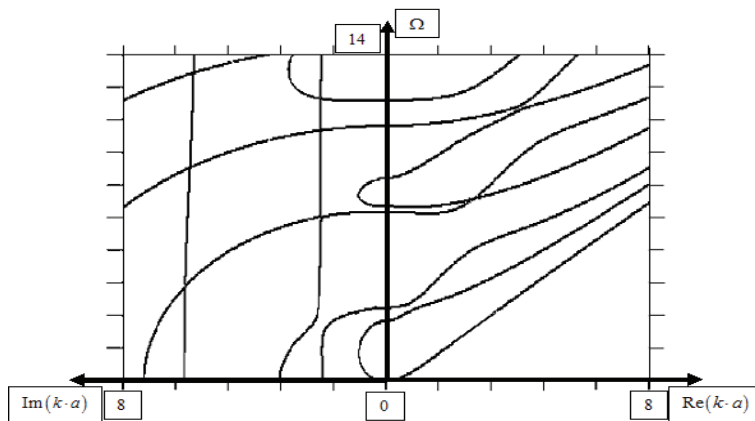


Fig. 2. PZT-4 cylinder with open-circuit lateral surface ( $m = 1$ )

Dispersion curves of bending waves ( $m = 1$ ) in the cylinder made from PZT-4 with the open-circuit lateral surface are demonstrated in Fig. 2. It is obvious that the electric boundary conditions substantially influence both propagating and evanescent waves. For example, in the case of the open-circuit lateral surface the dispersion curves are even steeper than the corresponding curves in the case of the short-circuit lateral surface.

In Fig. 3 a conceptual case of reduced electro-mechanical coupling coefficients ( $e_{15} = e_{31} = 0, e_{33} = 10^{-3} e_{33(PZT-4)}$ ) is shown.

In Fig. 4 and 5 the dispersion curves of PZT-7A material are presented for the open- and short-circuit lateral surfaces respectively.

In comparison with PZT-4 this material has lower values of the electro-mechanical coupling coefficients but practically the same elastic coefficients and mass density.

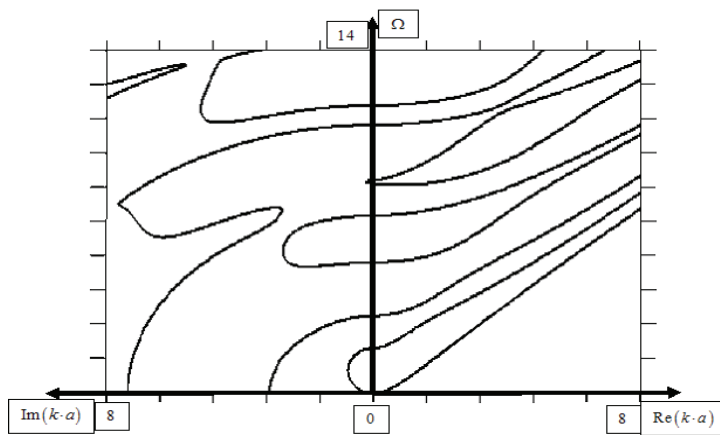
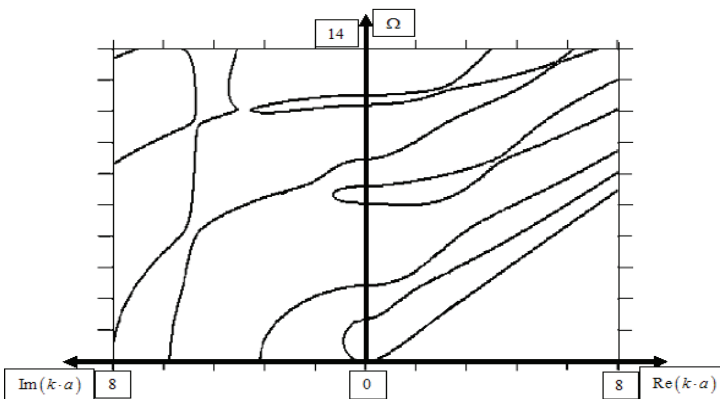


Fig. 3. PZT-4 cylinder with reduced electro-mechanical coupling

$$(m = 1, e_{15} = e_{31} = 0, e_{33} = 10^{-3}e_{33(\text{PZT-4})})$$


 Fig. 4. PZT-7A cylinder with short-circuit lateral surface ( $m = 1$ )

It follows from Fig. 1 - 5 that the first fundamental mode of the bending waves is not sensitive to the nature of the electric boundary conditions on the lateral cylindrical surface. Furthermore it is practically not sensitive to the measure of electro-mechanical coupling of the material. The higher order modes are more sensitive to the nature of the electric boundary condition as well as to the measure of the electro-mechanical cross-coupling. Fig. 3 - 5 shows that dispersion curves differ quite substantially from the curves in Fig. 1 and 2. This difference is explained mainly by the factor that the electro-mechanical coupling coefficients of PZT-7A are less than the corresponding factors of PZT-4. It is reflected in undulating behaviour of the propagating higher modes as well as the values of the cut-off frequencies. The PZT-4 cylinder with short-circuit lateral surface demonstrates a negative slope of the fourth branch in a quite broad range of wavenumbers (Fig. 1). Substantial

dependence of dispersion curves on electric boundary conditions is obvious from the behaviour of the curves for the evanescent waves.

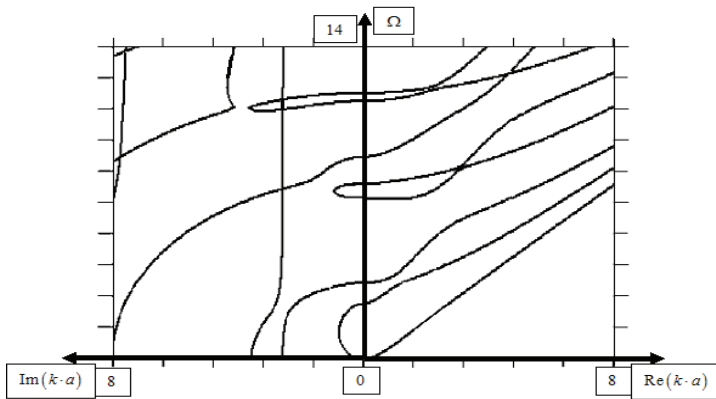


Fig. 5. PZT-7A cylinder with open-circuit lateral surface ( $m = 1$ )

Dispersion curves of non-axisymmetric waves with the circumferential wavenumber  $m = 2$  in the cylinders made from PZT-4 and PZT-7A with the open- and close-circuit lateral surface are depicted in Fig. 6 - 9. Again as for the case  $m = 1$  the substantial difference in the dispersion curves behaviour is explained by different types of the electric boundary conditions as well as by the difference in the electro-mechanic coupling coefficients.

Dispersion curves of non-axisymmetric waves with the circumferential wavenumber  $m = 3$  in the cylinder made from PZT-4 and PZT-7A with the open- and close-circuit lateral surface are depicted in Fig. 10-13.

The dispersion curves of higher circumferential wavenumbers ( $m = 2, 3$ ) are sensitive to the nature of the electric boundary condition as well as to the measure of the electro-mechanical cross-coupling for both propagating and evanescent waves. These dispersions curves obtained from the exact solution of the problem could be used as references data for developing of reliable finite elements for approximate solution of the problems of wave propagation in piezoelectric structures.

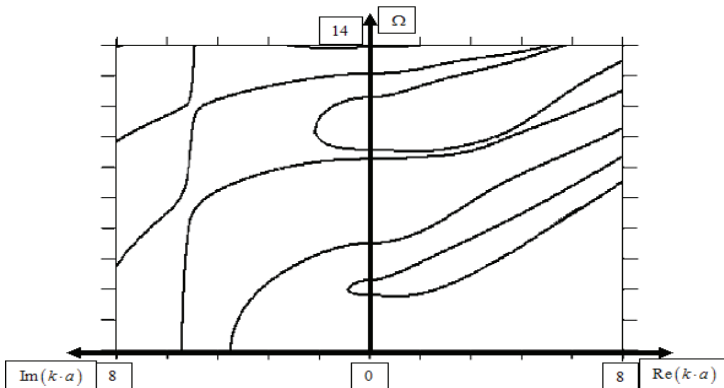


Fig. 6. PZT4 cylinder with short-circuit lateral surface ( $m = 2$ )

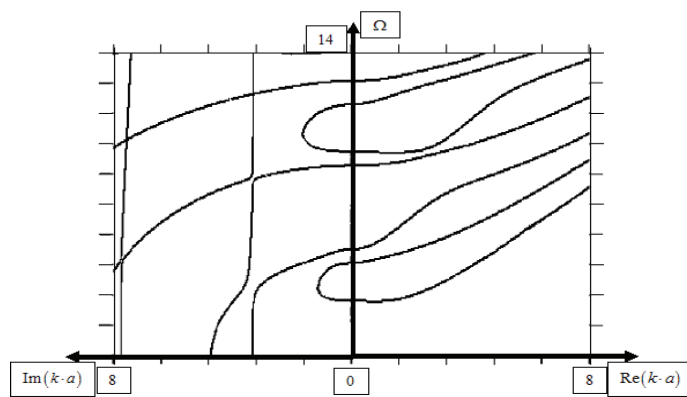


Fig. 7. PZT4 cylinder with open-circuit lateral surface ( $m = 2$ )

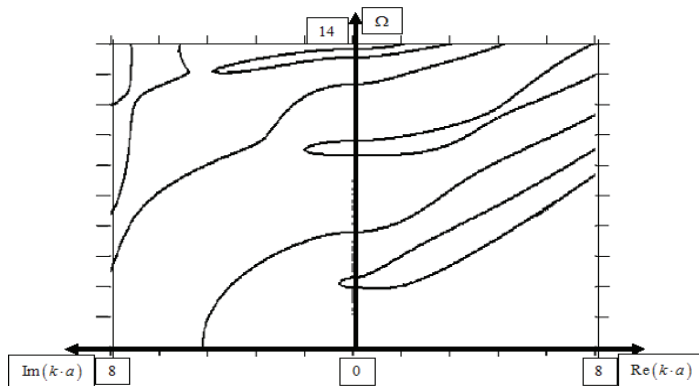


Fig. 8. PZT7A cylinder with short-circuit lateral surface ( $m = 2$ )

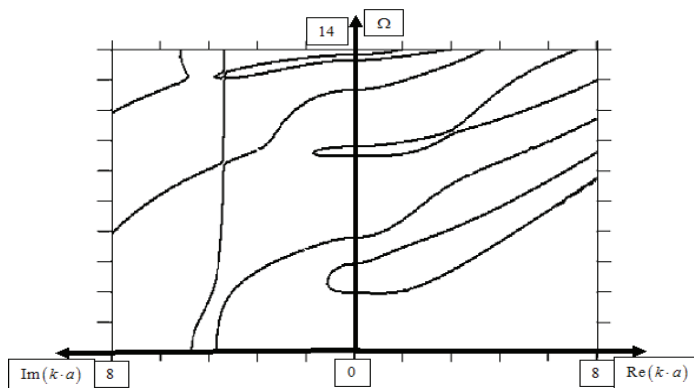


Fig. 9. PZT7A cylinder with open-circuit lateral surface ( $m = 2$ )

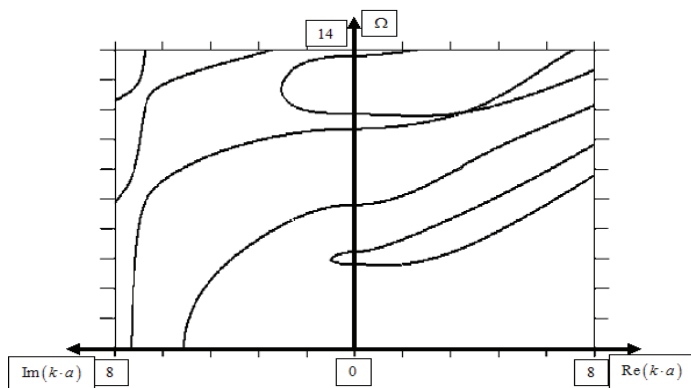


Fig. 10. PZT-4 cylinder with short-circuit lateral surface ( $m = 3$ )

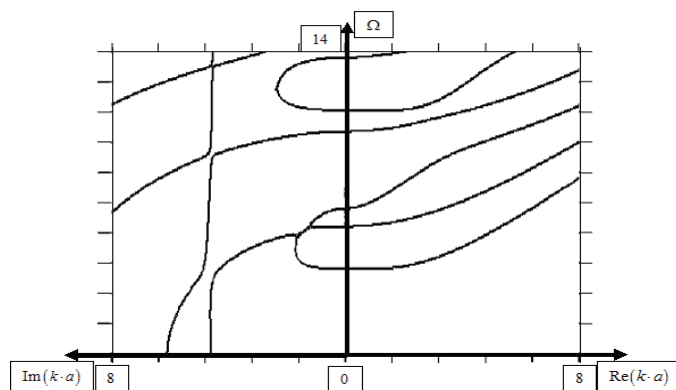


Fig. 11. PZT-4 cylinder with open-circuit lateral surface ( $m = 3$ )

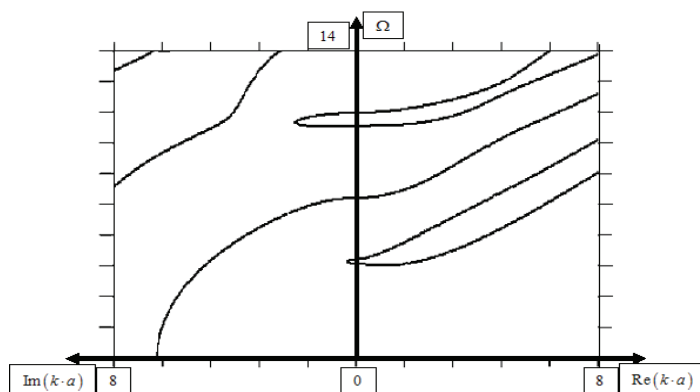


Fig. 12. PZT-7A cylinder with short-circuit lateral surface ( $m = 3$ )

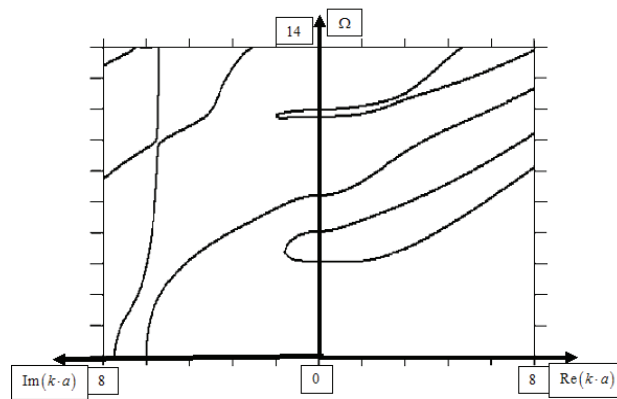


Fig. 13. PZT-7A cylinder with open-circuit lateral surface ( $m = 3$ )

Dispersion curves of axisymmetric waves in the cylinder made from PZT-4 and PZT-7A with the short-circuit and free lateral (cylindrical) surface are depicted in Fig. 14 - 17 in the same dimensionless coordinates  $(k \cdot a \div \Omega = \omega / (a \cdot V_s))$ , where  $V_s = \sqrt{c_{44}^E / \rho}$ , and  $a$  is the outer radius of the cylinder. The picture of the dispersion curves is obtained by a method described above for real (propagating waves) and pure imaginary values of the wavenumber in the limits:  $\text{Re}(k \cdot a), \text{Im}(k \cdot a) \in (0, 8]$ ,  $\Omega = \omega / (a \cdot V_s) \in (0, 28]$  with resolution 500 (250 pixels for real and 250 pixels for imaginary  $(k \cdot a)$ )  $\times$  250 ( $\Omega = \omega / (a \cdot V_s)$ ) pixels.

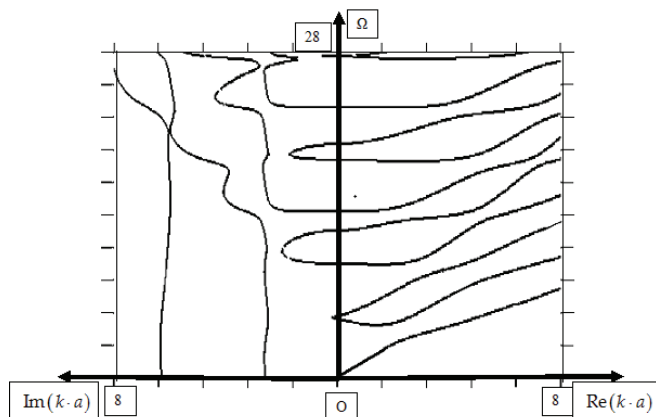


Fig. 14. Axisymmetric dispersion curves in PZT-4 cylinder with short-circuit lateral surface

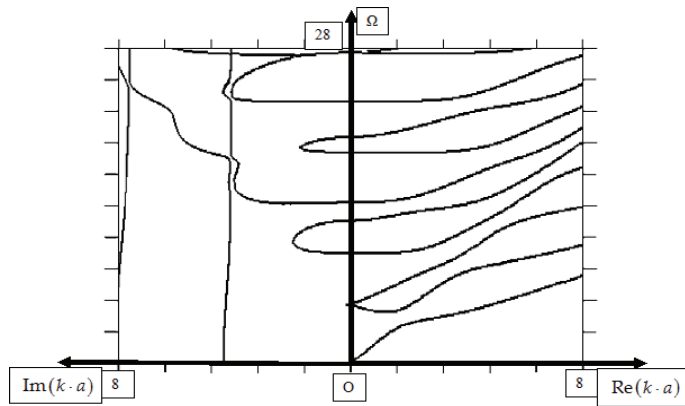


Fig. 15. Axisymmetric dispersion curves in PZT-4 cylinder with open-circuit lateral surface

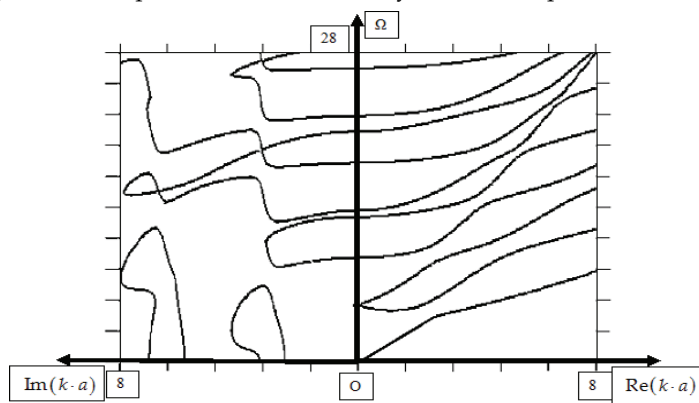


Fig. 16. Axisymmetric dispersion curves in PZT-7A cylinder with short-circuit lateral surface

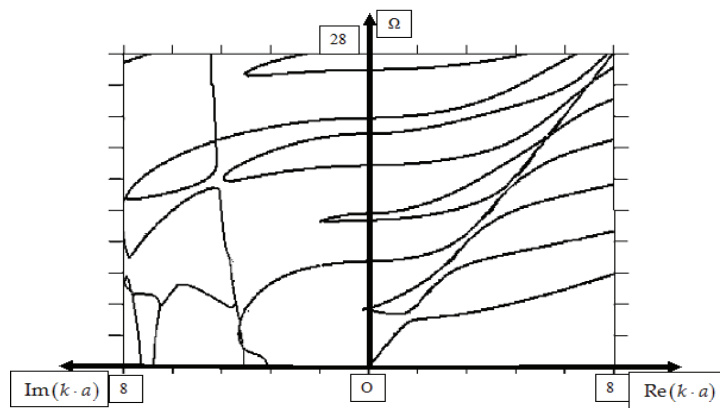


Fig. 17. Axisymmetric dispersion curves in PZT-7A cylinder with open-circuit lateral surface

## Appendix

Coefficients of main determinant (38) for the case  $\operatorname{Re}(\xi_j) \neq 0$ , ( $j = 0, 1, 2, 3$ ):

$$\begin{aligned}
 a_{11} &= \frac{2\xi_1 c_{66}^E}{a} J_{m+1}(\xi_1 a) + \left[ i k (\eta_1 c_{13}^E + \mu_1 e_{13}) - \xi_1^2 c_{13}^E + \frac{2c_{66}^E}{a^2} m(m-1) \right] J_m(\xi_1 a), \\
 a_{21} &= - \left[ (\eta_1 + ik) c_{44}^E + \mu_1 e_{15} \right] \left[ \xi_1 J_{m+1}(\xi_1 a) - \frac{m}{a} J_m(\xi_1 a) \right], \\
 a_{31} &= \frac{2mc_{66}^E}{a} \left[ \xi_1 J_{m+1}(\xi_1 a) - \frac{m-1}{a} J_m(\xi_1 a) \right], \\
 a_{12} &= \frac{2\xi_2 c_{66}^E}{a} J_{m+1}(\xi_2 a) + \left[ i k (\eta_2 c_{13}^E + \mu_2 e_{13}) - \xi_2^2 c_{13}^E + \frac{2c_{66}^E}{a^2} m(m-1) \right] J_m(\xi_2 a), \\
 a_{22} &= - \left[ (\eta_2 + ik) c_{44}^E + \mu_2 e_{15} \right] \left[ \xi_2 J_{m+1}(\xi_2 a) - \frac{m}{a} J_m(\xi_2 a) \right], \\
 a_{32} &= \frac{2mc_{66}^E}{a} \left[ \xi_2 J_{m+1}(\xi_2 a) - \frac{m-1}{a} J_m(\xi_2 a) \right], \\
 a_{13} &= \frac{2\xi_3 c_{66}^E}{a} J_{m+1}(\xi_3 a) + \left[ i k (\eta_3 c_{13}^E + \mu_3 e_{13}) - \xi_3^2 c_{13}^E + \frac{2c_{66}^E}{a^2} m(m-1) \right] J_m(\xi_3 a), \\
 a_{23} &= - \left[ (\eta_3 + ik) c_{44}^E + \mu_3 e_{15} \right] \left[ \xi_3 J_{m+1}(\xi_3 a) - \frac{m}{a} J_m(\xi_3 a) \right], \\
 a_{33} &= \frac{2mc_{66}^E}{a} \left[ \xi_3 J_{m+1}(\xi_3 a) - \frac{m-1}{a} J_m(\xi_3 a) \right], \\
 a_{14} &= - \frac{2mc_{66}^E}{a} \left[ \xi_0 J_{m+1}(\xi_0 a) - \frac{m-1}{a} J_m(\xi_0 a) \right], \\
 a_{24} &= - \frac{imkc_{44}^E}{a} J_m(\xi_0 a), \\
 a_{34} &= - \frac{2c_{66}^E}{a} \left[ \xi_0 J_{m+1}(\xi_0 a) - \left( \frac{\xi_0^2}{2} - \frac{m(m-1)}{a^2} \right) J_m(\xi_0 a) \right].
 \end{aligned}$$

For electric boundary condition  $D_1|_{r=a} = 0$ , ( $\operatorname{Re}(\xi_j) \neq 0$ ):

$$\begin{aligned}
 a_{41} &= - \left[ (\eta_1 + ik) e_{15} - \mu_1 \varepsilon_{11}^S \right] \left[ \xi_1 J_{m+1}(\xi_1 a) - \frac{m}{a} J_m(\xi_1 a) \right], \\
 a_{42} &= - \left[ (\eta_2 + ik) e_{15} - \mu_2 \varepsilon_{11}^S \right] \left[ \xi_2 J_{m+1}(\xi_2 a) - \frac{m}{a} J_m(\xi_2 a) \right],
 \end{aligned}$$

$$a_{43} = -\left[ (\eta_3 + ik)e_{15} - \mu_3 c_{11}^E \right] \left[ \xi_3 J_{m+1}(\xi_3 a) - \frac{m}{a} J_m(\xi_3 a) \right],$$

$$a_{44} = -\frac{imk e_{15}}{a} J_m(\xi_0 a).$$

For electric boundary condition  $\phi|_{r=a} = 0$ ,  $(\operatorname{Re}(\xi_j) \neq 0)$ :

$$a_{41} = \mu_1 J_m(\xi_1 a), \quad a_{42} = \mu_2 J_m(\xi_2 a), \quad a_{43} = \mu_3 J_m(\xi_3 a), \quad a_{44} = 0.$$

Coefficients of main determinant (38) for the case  $\operatorname{Re}(\xi_j) = 0$ ,  $(j = 0, 1, 2, 3)$ :

$$a_{11} = -\frac{2|\xi_1| c_{66}^E}{a} I_{m+1}(|\xi_1| a) + \left[ ik(\eta_1 c_{13}^E + \mu_1 e_{13}) + |\xi_1|^2 c_{13}^E + \frac{2c_{66}^E}{a^2} m(m-1) \right] I_m(|\xi_1| a),$$

$$a_{21} = \left[ (\eta_1 + ik)c_{44}^E + \mu_1 e_{15} \right] \left[ |\xi_1| I_{m+1}(|\xi_1| a) + \frac{m}{a} I_m(|\xi_1| a) \right],$$

$$a_{31} = -\frac{2mc_{66}^E}{a} \left[ |\xi_1| I_{m+1}(|\xi_1| a) + \frac{m-1}{a} I_m(|\xi_1| a) \right],$$

$$a_{12} = -\frac{2|\xi_2| c_{66}^E}{a} I_{m+1}(|\xi_2| a) + \left[ ik(\eta_2 c_{13}^E + \mu_2 e_{13}) + |\xi_2|^2 c_{13}^E + \frac{2c_{66}^E}{a^2} m(m-1) \right] I_m(|\xi_2| a),$$

$$a_{22} = \left[ (\eta_2 + ik)c_{44}^E + \mu_2 e_{15} \right] \left[ |\xi_2| I_{m+1}(|\xi_2| a) + \frac{m}{a} I_m(|\xi_2| a) \right],$$

$$a_{32} = -\frac{2mc_{66}^E}{a} \left[ |\xi_2| I_{m+1}(|\xi_2| a) + \frac{m-1}{a} I_m(|\xi_2| a) \right],$$

$$a_{13} = -\frac{2|\xi_3| c_{66}^E}{a} I_{m+1}(|\xi_3| a) + \left[ ik(\eta_3 c_{13}^E + \mu_3 e_{13}) + |\xi_3|^2 c_{13}^E + \frac{2c_{66}^E}{a^2} m(m-1) \right] I_m(|\xi_3| a),$$

$$a_{23} = \left[ (\eta_3 + ik)c_{44}^E + \mu_3 e_{15} \right] \left[ |\xi_3| I_{m+1}(|\xi_3| a) + \frac{m}{a} I_m(|\xi_3| a) \right],$$

$$a_{33} = -\frac{2mc_{66}^E}{a} \left[ |\xi_3| I_{m+1}(|\xi_3| a) + \frac{m-1}{a} I_m(|\xi_3| a) \right],$$

$$a_{14} = \frac{2mc_{66}^E}{a} \left[ |\xi_0| I_{m+1}(|\xi_0| a) + \frac{m-1}{a} I_m(|\xi_0| a) \right],$$

$$a_{24} = \frac{imk c_{44}^E}{a} I_m(|\xi_0| a),$$

$$a_{34} = \frac{2c_{66}^E}{a} \left[ |\xi_0| I_{m+1}(|\xi_0| a) - \left( \frac{|\xi_0|^2}{2} + \frac{m(m-1)}{a^2} \right) I_m(|\xi_0| a) \right].$$

For electric boundary condition  $D_1|_{r=a} = 0$ ,  $(\operatorname{Re}(\xi_j) = 0)$ :

$$a_{41} = [(\eta_1 + ik)e_{15} - \mu_1 \varepsilon_{11}^S] \left[ |\xi_1| I_{m+1}(|\xi_1|a) + \frac{m}{a} I_m(|\xi_1|a) \right],$$

$$a_{42} = [(\eta_2 + ik)e_{15} - \mu_2 \varepsilon_{11}^S] \left[ |\xi_2| I_{m+1}(|\xi_2|a) + \frac{m}{a} I_m(|\xi_2|a) \right],$$

$$a_{43} = [(\eta_3 + ik)e_{15} - \mu_3 \varepsilon_{11}^S] \left[ |\xi_3| I_{m+1}(|\xi_3|a) + \frac{m}{a} I_m(|\xi_3|a) \right],$$

$$a_{44} = \frac{imke_{15}}{a} I_m(|\xi_0|a).$$

For electric boundary condition  $\phi|_{r=a} = 0$ ,  $(\operatorname{Re}(\xi_j) = 0)$ :

$$a_{41} = \mu_1 I_m(|\xi_1|a), \quad a_{42} = \mu_2 I_m(|\xi_2|a), \quad a_{43} = \mu_3 I_m(|\xi_3|a), \quad a_{44} = 0.$$

In the axisymmetric case we assume  $m=0$  in the above mentioned expressions and remove third row and fourth column in determinant (37).

## 7. Conclusion

The characteristic equation of non-axisymmetric propagating and evanescent waves of a piezoelectric cylinder of transversely isotropic material was developed. The results were numerically illustrated for sample PZT-4 and PZT-7A cylinders for the first three circumferential wavenumbers ( $m = 1, 2, 3$ ) and for the axisymmetric case. It was shown that the dispersion curves are sensitive both to the electric boundary conditions and to the measure of electro-mechanical coupling. This effect was revealed more strongly in the higher order modes.

## 8. Acknowledgements

I acknowledge the support of my co-authors Prof. Arthur G. Every and our student Alfred S. Yenwong-Fai participating in the investigation of the non-axisymmetric case of the piezoelectric cylinder vibrations (Shatalov, et al. 2009). I also want to thank Mr. Yuri M. Shatalov who investigated the axisymmetric case under my supervision.

## 9. References

- Achenbach, J. (1984). *Wave Propagation in Elastic Solids*, New York, North-Holland
- Armenakas, A. & Reitz, E. (1973). Propagation of harmonic waves in orthotropic circular cylindrical shells, *J. Appl. Mech.* 40, 168-174
- Bai, H.; Shah, A.; Dong, S. & Taciroglu, E. (2006). End reflections in layered piezoelectric circular cylinder. *International Journal of Solids and Structures*, 43, 6309-6325.
- Bai, H.; Taciroglu, E.; Dong, S. & Shah, A., (2004). Elastodynamic Green's function for a laminated piezoelectric cylinder, *International Journal of Solids and Structures*, 41, 6335-6350

- Berliner, M. & Solecki, R. (1996). Wave propagation in fluid-loaded transversely isotropic cylinders. Part 1. Analytical formulation, *J. Acoust. Soc. Am.*, 99, 1841-1847
- Chree, C. (1890). *Q. J. Math.*, 24, 340-354.
- Crandall, S.; Karnop, E.; Kurtz, J. & Pridemore-Brown, D. (1968). *Dynamics of Mechanical and Electromechanical Systems*, Krieger Publishing Co, Malabar, Florida
- Every A., & Neiman V. (1992). Reflection of electroacoustic waves in piezoelectric solids: Mode conversion into four bulk waves, *J. Appl. Phys.* 71, 6018-6024
- Frazer, W. (1980). Separable equations for a cylindrical anisotropic elastic waveguide, *J. Sound Vib.* 72, 151-157
- Graff, K. (1991). *Wave Motion in Elastic Solids*, New York: Dover
- Hagood, N.; Chung, W. & Flotow, A. (1990). Modelling of piezoelectric actuator dynamics for active structural control, *J. of Intell. Mater. Syst. And Struct.* 1 (3), 327-354
- Honarvar, F.; Enjilela, E. & Sinclair, A. (2008). An alternative method for plotting dispersion curves, *Ultrasonics*, doi:10.1016/j.ultras.2008.07.002
- Honarvar, F.; Enjilela, E.; Sinclair, A. & Minerzami, S. (2007). Wave propagation in transversely isotropic cylinders, *International Journal of Solids and Structures*, 44, 5236-5246
- Mirsky, I. (1964). Wave propagation in transversely isotropic circular cylinders. Part 1: Theory, *J. Acoust. Soc. Am.* 36, 2106-2122
- Nayfeh, A.; Abdelrahman, W. & Nagy, P. (2000). Analysys of axisymmetric waves in layered piezoelectric rods and their composites, *J. Acoust. Soc. Am.* 108 (4), 1496-1504
- Nayfeh, A. & Nagy, P. (1995). General study of axisymmetric waves in layered anisotropic fibres and their composites, *J. Acoust. Soc. Am.*, 99, 931-941
- Niklasson, A. & Datta, S. (1998). Scattering by an infinite transversely isotropic cylinder in a transversely isotropic medium, *Wave motion*, 27 (2), 169-185
- Paul, H. (1966). Vibrations of circular cylindrical shells of piezoelectric silver iodide crystals, *J. Acoust. Soc. Am.* 40, 1077-1080
- Pochhammer, L. (1876). *J. reine angew. Math.* 81, 324
- Rose, J. (1999). *Ultrasonic Waves in Solid Media*, Cambridge University Press
- Shatalov, M. & Loveday, P. (2004). Electroacoustic wave propagation in transversely isotropic piezoelectric cylinders, *Proceedings of the South African Conference on Applied Mechanics (SACAM04)*
- Shatalov, et al. (2009). Analysis of non-axisymmetric wave propagation in a homogeneous piezoelectric solid circular cylinder of transversely isotropic material, *International Journal of Solids and Structures* 46, 837-850
- Siao, J.; Dong, S. & Song, J. (1994). Frequency spectra of laminated piezoelectric cylinders, *ASME Journal of Vibrations and Acoustics*, 116, 364-370
- Wei, J., Su, X., 2005. Wave propagation in a piezoelectric rod of 6mm symmetry. *International Journal of Solids and Structures*, 42, 3644-3654
- Winkel, V.; Oliveira, J.; Dai, J. & Jen, C. (1995). Acoustic wave propagation in piezoelectric fibres of hexagonal crystall symmetry, *IEEE Trans. Ultrason. Ferroelectr. Freq. Control*, 42, 949-955
- Xu, P. & Datta, S. (1991). Characterization of fibre-matrix interface by guided waves: Axisymmetric case, *J. Acoust. Soc. Am.* 89 (6), 2573-2583
- Yenwong-Fai, A. (2008). Wave propagation in a piezoelectric solid cylinder of transversely isotropic material, *Master's thesis*, University of Witwatersrand, Johannesburg, South Africa